Supplemental Data

Structural basis for dual roles of Aar2p in U5 snRNP assembly

Gert Weber[1,*], Vanessa F. Cristão[2], Karine F. Santos[1], Sina Mozaffari Jovin[3], Anna C. Heroven[1], Nicole Holton[1], Reinhard Lührmann[3], Jean D. Beggs[2] and Markus C. Wahl[1,*]

[1] Freie Universität Berlin, Fachbereich Biologie/Chemie/Pharmazie, Abteilung Strukturbiochemie, Takustraße 6, D-14195 Berlin, Germany

[2] Wellcome Trust Centre for Cell Biology, University of Edinburgh, Edinburgh, EH9 3JR, UK

[3] Max-Planck-Institut für biophysikalische Chemie, Zelluläre Biochemie, Am Faßberg 11, D-37077 Göttingen, Germany

[*] **Corresponding authors**

Gert Weber
Tel.: +49 30 838 57359
Fax: +49 30 838 56981
eMail: gweber@chemie.fu-berlin.de

Markus C. Wahl
Tel: +49 30 838 53456
Fax: +49 30 838 56981
eMail: mwahl@zedat.fu-berlin.de

Supplemental Materials and Methods

Cloning, expression and protein purification

Plasmids for the production of RH (Prp8p residues 1836-2092), Jab1 (Prp8p residues 2147-2413), Aar2p and Aar2p$^{1-331}$ have been described elsewhere (Pena et al. 2008; Pena et al. 2009; Weber et al. 2011). A DNA fragment encoding Jab1 including the preceding RH-Jab1 linker (Prp8p residues 2093-2413) was cloned into pETM-11 to yield a protein with a TEV-cleavable N-terminal His$_6$-tag (Jab1^{linker}). The coding region for Prp8p CTF (Prp8p residues 1836-2413) was cloned into pGEX-6p for expression with a PreScission-cleavable N-terminal GST-tag. A DNA fragment encoding Aar2p$^{\Delta loop}$ (Aar2p residues 153-170 replaced by five serine residues) was cloned into pETM-13 for production with a C-terminal His$_6$-tag. The open reading frame of Aar2p$^{\Delta loop}$ followed by a stop codon was cloned into pETM-13, to yield an untagged Aar2p$^{\Delta loop}$ protein. The coding region of Aar2p$^{\Delta loop}$, residues 1-318, was cloned into pETM-13 to produce Aar2p$^{1-318,\Delta loop}$ with a C-terminal His$_6$-tag. Mutagenesis was performed with the QuikChange site-directed mutagenesis kit (Stratagene).

For protein production, *E. coli* Rosetta2 (DE3) cells were transformed with the respective plasmids, grown in terrific broth to an OD_{600} of 0.6 at 37 °C, cooled to 20 °C, induced with 0.5 mM IPTG and incubated at 20 °C over night. Cells were harvested by centrifugation and stored at -80 °C. Cell pellets from expression cultures were resuspended in lysis buffer (20 mM Tris-HCl, pH 7.5, 150 mM NaCl, 1 mM DTT) in the presence of a protease inhibitor cocktail (Roche). Cells were lyzed using a Sonoplus sonifier (Bandelin) and cell debris were removed by centrifugation.

For purification of Aar2p bearing a C-terminal His$_6$-tag, Aar2p$^{1-331}$, Aar2p$^{1-318,\Delta loop}$, RH, Jab1, Jab1^{linker} and mutants of these proteins, the soluble extracts were passed over a Ni^{2+}-NTA gravity flow column, pre-equilibrated with lysis buffer. The beads were washed with lysis buffer, containing 30 mM imidazole. Proteins were eluted with lysis buffer supplemented with 300 mM imidazole. The Ni^{2+}-NTA eluate of Aar2p or its mutants were further purified *via* Superdex 75 gel filtration chromatography (GE Healthcare) in lysis buffer. Peak fractions

were pooled, concentrated to 10-30 mg/ml, flash frozen in liquid nitrogen and stored at -80 °C. The Ni^{2+}-NTA eluates of RH, Jab1, $Jab1^{linker}$ or their mutants were cleaved by TEV protease to remove the N-terminal His_6-tags. The untagged proteins were further purified by Superdex 75 size exclusion chromatography in lysis buffer. Residual contaminants were removed by passing the peak fractions again over Ni^{2+}-NTA agarose. The purified proteins were concentrated to 10-25 mg/ml, flash frozen in liquid nitrogen and stored at -80 °C.

The soluble fraction of the GST-CTF cell lysate was passed over a glutathione sepharose gravity flow column. The beads were washed with lysis buffer and GST-CTF was eluted with lysis buffer containing 10 mM reduced glutathione. The eluate was treated with PreScission protease to remove the GST-tag and further purified by Superdex 75 size exclusion chromatography. The peak fractions of CTF were pooled and concentrated to 10-30 mg/ml, flash frozen in liquid nitrogen and stored at -80 °C.

For production of the $Aar2p^{\Delta loop}$-RH-Jab1 complex, the cleared cell lysate from a co-expression culture of $Aar2p^{\Delta loop}$ and RH were mixed and purified by Ni^{2+}-NTA agarose, TEV cleavage and size exclusion chromatography as described above. The peak fractions of the $Aar2p^{\Delta loop}$-RH complex were pooled, concentrated and mixed with a twofold molar excess of pre-purified Jab1 protein. The mixture was subjected to Superdex 200 size exclusion chromatography (GE Healthcare) in lysis buffer. Peak fractions of the $Aar2p^{\Delta loop}$-RH-Jab1 complex were pooled, concentrated to 30 mg/ml, flash frozen in liquid nitrogen and stored at -80 °C.

Proteins designated for ITC were buffer exchanged to ITC buffer (20 mM Tris-HCl, pH 7.5, 150 mM NaCl) by Superdex 75 size exclusion chromatography or by desalting columns (PD10, GE Healthcare). Peak fractions were pooled, concentrated to 5-30 mg/ml, flash frozen in liquid nitrogen and stored at -80 °C. A synthetic C-terminal Aar2p peptide (residues 331-355; N-terminus acetylated) used in ITC was obtained from the Molecular Libraries and Recognition Group, Institute for Medical Immunology, Charité – University Medicine Berlin) and dissolved in ITC buffer.

Protein concentrations were determined *via* their absorbance at 280 nm using a NanoDrop UV-Vis Spectrophotometer (Thermo Scientific) and applying their calculated molar extinction coefficients (http://web.expasy.org/protparam; Supplemental Table S2).

Fluorescence-based thermal unfolding assay

Folding of all wt and mutant proteins employed herein was tested using a fluorescence-based thermal unfolding assay (Niesen et al. 2007). The experiments were carried out in a 96-well plate using a plate reader combined with a real-time PCR cycler (Mx3005P, Stratagene). Proteins were diluted in 20 mM Tris-HCl pH 7.5, 150 mM NaCl, 1 mM DTT supplemented with 10 x SYPRO orange (1:500 dilution of the stock; Invitrogen) in a total volume of 20 µl. Protein concentrations in the assays were 0.1 mg/ml for Brr2p, 0.2 mg/ml for Jab1 and RH variants and 0.3 mg/ml for all other proteins. The temperature was ramped from 25 °C to 95 °C in steps of 1 °C/min with intervals of 30 sec between steps and the fluorescence emission at 610 nm was monitored at each step. Fluorescence intensities were corrected for the background signal of the fluorophore in buffer, plotted as a function of temperature and the thermal melting temperatures (T_m) were deduced from the inflection points on the ascending branches of the curves.

Analytical gel filtration chromatography

Single proteins and protein mixtures were analyzed by analytical size exclusion chromatography on a Superdex 200 PC3.2 column (GE Healthcare) in size exclusion buffer (20 mM Tris-HCl, pH 7.5, 150 mM NaCl, 0.5 mM DTT) at a flow rate of 50-70 µl/min. The gel filtration column was calibrated with a mixture of bovine γ-globulin (158 kDa), chicken ovalbumin (44 kDa) and horse myoglobin (17 kDa). The resolution of the column was determined at 15,288 plates/m. For analysis of complex formation, proteins were mixed in estimated equimolar ratios relative to 50 µg Brr2 (for all runs containing Brr2), 20 µg RH (for all runs containing Jab1 and mutant Jab1 proteins) or 10 µg RH (for all other runs) in 55 µl size exclusion buffer. In the case of Aar2p-RH-Jab1 interaction tests, Aar2p (or Aar2p

variants) was first mixed with RH and incubated for 2 min on ice before addition of Jab1 (or Jab1 variants). For Brr2p-CTF-Aar2p interaction tests, Aar2p (or Aar2p variants) was first mixed with CTF (or CTF variants) and incubated for 2 min on ice before addition of Brr2p. Protein mixtures were incubated for 30 min on ice before loading on the column. Eluted fractions were analyzed by SDS-PAGE. In these experiments, we used Aar2p bearing a C-terminal His_6-tag.

Crystallographic analyses

For crystallization, we used untagged Aar2p$^{\Delta loop}$ or Aar2p$^{1-331}$ and Aar2p$^{1-318,\Delta loop,S253E}$ bearing a C-terminal His_6-tag. Proteins and complexes were crystallized by sitting drop vapor diffusion (1 µl protein complex plus 1 µl reservoir) at 4 °C (Aar2p$^{\Delta loop}$-RH-Jab1 complex, Aar2p$^{1-331}$-RH complex) or 20 °C (Aar2p$^{1-318,\Delta loop,S253E}$). The Aar2p$^{\Delta loop}$-RH-Jab1 complex crystallized with a reservoir containing 0.1 M HEPES-NaOH, pH 7.5, 12 % (w/v) PEG 6000 and 0.6 M KCl. Crystals were cryo-protected by transfer into 20 % PEG 400 and 150 mM NaCl. The Aar2p$^{1-331}$-RH complex crystallized with a reservoir containing 0.1 M Tris-HCl, pH 8.0, 19 % (w/v) PEG 4000 and 100 mM KCl. Crystals were cryo-protected by transfer into perfluoro polyether. Aar2p$^{1-318,\Delta loop,S253E}$ crystallized with a reservoir containing 40 mM imidazole, pH 7.75, 0.95 M sodium potassium tartrate and 0.2 M sodium chloride. Crystals were cryo-protected by transfer into 150 mM NaCl and 25 % (v/v) glycerol. RH^{W1911A} was crystallized and cryo-protected as described in (Pena et al. 2008) for the wt protein. All crystals were incubated in the respective cryo-protecting solution or oil for 10-30 s and then flash-cooled in liquid nitrogen. Diffraction data were collected at 100 K on beamline 14.2 of the BESSY II storage ring (Berlin, Germany). All diffraction data were processed with XDS (Kabsch 1993).

The structure of the Aar2p$^{\Delta loop}$-RH-Jab1 complex was solved by molecular replacement using the program PHASER (McCoy 2007) and the structure coordinates of RH (PDB IDs 3E9O and 3E9P; (Pena et al. 2008)), Jab1 (PDB ID 2OG4; (Pena et al. 2007)) and Aar2p^{Subt} derived from the Aar2p^{Subt}-RH complex (PDB ID 3SBT; (Weber et al. 2011)). The initial

electron density was of good quality and allowed the building of all Aar2p$^{\Delta loop}$ residues except for a short region (residues 318-338) preceding its C-terminus. The structure of the Aar2p$^{1-331}$-RH complex was solved by molecular replacement with PHASER and the structure coordinates of the Aar2p^{Subt}-RH complex (PDB ID 3SBT; (Weber et al. 2011)). The structure of RH^{W1911A} was solved by molecular replacement with PHASER employing the structure coordinates of RH (PDB ID 3E9P; (Pena et al. 2008)). The structure of Aar2p$^{1-318,\Delta loop,S253E}$ was solved by molecular replacement with PHASER using the structure coordinates of Aar2p$^{\Delta loop}$ from the Aar2p$^{\Delta loop}$-RH-Jab1 complex. For the crystal packing function, PHASER was set to ignore clashes arising from conformational changes in the C-terminus of Aar2p$^{1-318,\Delta loop,S253E}$. During initial stages of refinement, residues 183-215 in the C-terminus of Aar2p$^{1-318,\Delta loop,S253E}$ were deleted and partially rebuilt into electron density accounting for the new conformation of this region. The structure was refined with NCS restraints on the two non-crystallographic copies in an asymmetric unit and strict restraints on geometry. NCS restraints were omitted during the final round of refinement. Structural models were completed through alternating rounds of automated refinement using PHENIX.REFINE (Zwart et al. 2008) and manual model building using COOT (Emsley and Cowtan 2004).

Isothermal titration calorimetry

For all ITC experiments, we used Aar2p and Aar2p mutant proteins bearing a C-terminal His_6-tag. Proteins were buffer exchanged to 20 mM Tris-HCl, pH 7.5, 150 mM NaCl and their concentrations were determined *via* the absorbance at 280 nm. ITC measurements were conducted at 25 °C on a MicroCal^{TM} iTC200 system (GE Healthcare), using the following setups: RH (141µM) as sample and Aar2p (12.6 µM) as titrant (16 injections of 2.5 µl each); CTF (102 µM) as sample and Aar2p (9.0 µM) as titrant (16 injections of 2 µl each); CTF (64 µM) as sample and Aar2p^{T345E} (12.6 µM) as titrant (16 injections of 2 µl each); CTF (56 µM) as sample and Aar2p^{S253E} (6.3 µM) as titrant (16 injections of 2 µl each); CTF (64 µM) as sample and Aar2p$^{S253E/T345E}$ (6.4 µM) as titrant (16 injections of 2 µl each); CTF (102 µM) as sample and Aar2p C-terminal peptide (10 µM) as titrant (16 injections of 2 µl each); Jab1 (22

µM) as a sample and Aar2p-RH (232 µM) as titrant (16 injections of 2.5 µl each); Jab1^{linker} (27 µM) as a sample and Aar2p-RH (240 µM) as titrant (16 injections of 2.5 µl each). Titrant heats of dilution were subtracted and data were fitted using MicroCal Origin 7.

Electrophoretic mobility shift assay

U4 and U6 snRNAs were *in vitro* transcribed by T7 RNA polymerase. U6 snRNA was 5'-end radiolabeled and annealed to the U4 snRNA, followed by purification of the U4/U6 di-snRNA by 6 % non-denaturing PAGE. For binding and competition experiments involving CTF, 1 nM of labeled U4/U6 were combined with 1 µM of CTF, Aar2p or premixed proteins in EMSA buffer (40 mM Tris-HCl, pH 7.5, 75 mM NaCl, 8 % (w/v) glycerol, 2.5 mM $MgCl_2$, 100 ng/µl acetylated BSA, 50 µg/ml *E. coli* tRNA and 1.5 mM DTT) and incubated for 30 min at 10 °C. For competition titrations, Aar2p was added at the indicated concentrations (0, 0.5, 1, 2, 3 or 5 µM) to CTF-U4/U6 complex prepared as above, and the mixtures were incubated for additional 30 min at 10 °C. For binding and competition experiments involving RH, 1 nM of labeled U4/U6 were combined with 2.5 µM of RH in EMSA buffer and incubated for 30 min at 10 °C. Subsequently, 5 µM of the indicated Aar2p variant was added and the mixtures were incubated for additional 30 min at 10 °C. RNA-protein (RNP) complexes were resolved on 6 % native polyacrylamide gels and visualized by autoradiography.

Testing the effects of phosphosite mutations in *AAR2* on growth of yeast cells

For over-production in yeast L40ΔG cells, *AAR2* or the phosphomutant alleles were expressed as LexA fusions in pBTM116 (Weber et al. 2011) along with Prp8p$^{1649-2413}$ (E1), Prp8p$^{2010-2413}$ (E3) or Prp8p$^{2010-2413,Y2037H/I2051T}$ (E3H) fragments previously cloned in pACTII-stop vector (van Nues and Beggs 2001). Ten-fold dilutions of cells were spotted on minimal dropout –LW agar plates and incubated at various temperatures.

To introduce the phosphosite mutations into the yeast genome, the sequences bearing the wt *AAR2* or phosphosite mutant alleles were copied from the corresponding pBTM116-*AAR2* plasmids (Weber et al. 2011) into pGID3 upstream of the Nat^R cassette (conferring

resistance to nourseothricin; (Decourty et al. 2008)). The *AAR2* sequences together with Nat^R were amplified by PCR and introduced into the genome of yeast W303 cells by homologous recombination and Nat^R selection. The presence of the mutations at the *AAR2* locus was confirmed by yeast colony PCR and DNA sequencing.

Supplemental Results

The internal Aar2p loop is not involved in interactions with CTF

In the Aar2p$^{\Delta loop}$-RH-Jab1 complex, the internal loop of Aar2p is positioned next to the palm of the RH domain (Fig. 1B). As we had obtained the present complex structure using a loop-exchanged variant of Aar2p, we directly tested whether the wt loop is involved in complex formation. We expressed and purified an Aar2p construct containing the wt internal loop but lacking the last 24 residues (Aar2p$^{1-331}$), co-crystallized the protein in complex with RH (Supplemental Fig. S5) and determined the structure using diffraction data to 1.85 Å resolution (Supplemental Table S1). The structure of the Aar2p$^{1-331}$-RH closely resembles the the reassigned structure of Aar2p^{Subt}-RH (overall rmsd 1.87 Å; rmsd Aar2p components 1.34 Å; rmsd RH components 2.10 Å) and the Aar2p$^{\Delta loop}$-RH sub-structure from the Aar2p$^{\Delta loop}$-RH-Jab1 complex (overall rmsd 4.26 Å; rmsd Aar2p components 1.72 Å; rmsd RH components 2.19 Å; Supplemental Fig. S5A and B). Although a large cavity in the crystal lattice of the Aar2p$^{1-331}$-RH complex would have allowed for the internal Aar2p loop to contact RH, no corresponding electron density developed during structure solution and refinement (Supplemental Fig. S5C). SDS PAGE analysis of dissolved crystals showed that the protein remained intact during crystallization (Supplemental Fig. S5D). As the internal Aar2p loop is also remote from Jab1 in the Aar2p$^{\Delta loop}$-RH-Jab1 complex (Fig. 1B), we conclude that it does not foster direct contacts to either Prp8p domain upon Aar2p binding.

Supplemental References

Barton, GJ. 1993. ALSCRIPT - A tool for multiple sequence alignments. *Protein Engineering* **6**: 37-40.

Davis, IW, Murray, LW, Richardson, JS, and Richardson, DC. 2004. MOLPROBITY: structure validation and all-atom contact analysis for nucleic acids and their complexes. *Nucl Acids Res* **32**: W615-619.

Decourty, L, Saveanu, C, Zemam, K, Hantraye, F, Frachon, E, Rousselle, JC, Fromont-Racine, M, and Jacquier, A. 2008. Linking functionally related genes by sensitive and quantitative characterization of genetic interaction profiles. *Proc Natl Acad Sci U S A* **105**: 5821-5826.

Emsley, P and Cowtan, K. 2004. Coot: model-building tools for molecular graphics. *Acta Crystallogr D* **60**: 2126-2132.

Hutchinson, EG and Thornton, JM. 1996. PROMOTIF--a program to identify and analyze structural motifs in proteins. *Protein Sci* **5**: 212-220.

Kabsch, W. 1993. Automatic processing of rotation diffraction data from crystals of initially unknown symmetry and cell constants. *J Appl Crystallogr* **26**: 795-800.

Larkin, MA, Blackshields, G, Brown, NP, Chenna, R, McGettigan, PA, McWilliam, H, Valentin, F, Wallace, IM, Wilm, A, Lopez, R et al. 2007. Clustal W and Clustal X version 2.0. *Bioinformatics* **23**: 2947-2948.

McCoy, AJ. 2007. Solving structures of protein complexes by molecular replacement with Phaser. *Acta Crystallogr D Biol Crystallogr* **63**: 32-41.

Niesen, FH, Berglund, H, and Vedadi, M. 2007. The use of differential scanning fluorimetry to detect ligand interactions that promote protein stability. *Nat Protoc* **2**: 2212-2221.

Pena, V, Jovin, SM, Fabrizio, P, Orlowski, J, Bujnicki, JM, Lührmann, R, and Wahl, MC. 2009. Common design principles in the spliceosomal RNA helicase Brr2 and in the Hel308 DNA helicase. *Mol Cell* **35**: 454-466.

Pena, V, Liu, S, Bujnicki, JM, Lührmann, R, and Wahl, MC. 2007. Structure of a multipartite protein-protein interaction domain in splicing factor prp8 and its link to retinitis pigmentosa. *Mol Cell* **25**: 615-624.

Pena, V, Rozov, A, Fabrizio, P, Lührmann, R, and Wahl, MC. 2008. Structure and function of an RNase H domain at the heart of the spliceosome. *EMBO J* **27**: 2929-2940.

van Nues, RW and Beggs, JD. 2001. Functional contacts with a range of splicing proteins suggest a central role for Brr2p in the dynamic control of the order of events in spliceosomes of Saccharomyces cerevisiae. *Genetics* **157**: 1451-1467.

Weber, G, Cristao, VF, de, LAF, Santos, KF, Holton, N, Rappsilber, J, Beggs, JD, and Wahl, MC. 2011. Mechanism for Aar2p function as a U5 snRNP assembly factor. *Genes Dev* **25**: 1601-1612.

Zwart, PH, Afonine, PV, Grosse-Kunstleve, RW, Hung, LW, Ioerger, TR, McCoy, AJ, McKee, E, Moriarty, NW, Read, RJ, Sacchettini, JC et al. 2008. Automated structure solution with the PHENIX suite. *Methods Mol Biol* **426**: 419-435.

Supplemental Tables

Supplemental Table S1. Crystallographic data and refinement[a]

	Aar2p$^{\Delta loop}$-RH-Jab1	**Aar2p$^{1-331}$-RH**	**RH^{W1911A}**	**Aar2p$^{1-318,\ \Delta loop,S253E}$**
Data Collection				
Wavelength (Å)	0.9184	0.9184	0.9184	0.9184
Temperature (K)	100	100	100	100
Space group	$P2_1$	C2	$P2_12_12_1$	$P3_221$
Unit cell parameters (Å, °)				
a/b/c	84.8/63.7/110.5	79.9/76.8/91.9	75.6/85.0/96.0	62.8/62.8/326.0
α/ß/γ	90/95.3/90	90/105.9/90	90/90/90	90/90/120
Resolution (Å)	34.3-2.1 (2.15-2.10)	35.0-1.85 (1.90-1.85)	50.0-2.0 (2.05-2.00)	50-3.2 (3.29-3.20)
Reflections				
Unique	68679 (5057)	45500 (3333)	42335 (3056)	13092 (920)
Completeness (%)	99.9 (99.7)	99.7 (100)	99.7 (99.6)	99.5 (98.6)
Redundancy	3.4 (3.5)	3.4 (3.4)	3.7 (3.7)	4.0 (4.1)
I/σ(I)	10.6 (1.6)	16.2 (2.0)	17.9 (2.6)	14.0 (2.0)
R_{sym}(I)[b]	0.08 (0.86)	0.07 (0.74)	0.05 (0.57)	0.10 (0.80)
Refinement				
Resolution (Å)	31.9-2.1	34.0-1.85	38.0-2.0	45.3-3.2
Reflections				
Number	68667	45500	42330	13090
Completeness (%)	99.7	99.8	99.7	99.6
Test set (%)	4.5	5.0	5.0	5.1
R_{work}[c]	0.180	0.168	0.180	0.260
R_{free}[c]	0.228	0.217	0.226	0.305
ESU (Å)[d]	0.29	0.24	0.21	0.44
Contents of A.U.[e]				
Proteins/residues	3/818	2/550	2/508	2/582
Water oxygens	689	513	366	-
HEPES	1	-	-	-
Mean B-factors (Å^2)				
Wilson	30.0	20.6	31.8	78.0
Protein	47.1	16.7	40.5	144.4
Solvent	48.9	26.6	44.3	-
Ramachandran plot[f] (%)				
Favored	97.0	97.2	97.6	95.3
Allowed	3.0	2.8	2.4	4.7
Outliers	-	-	-	-
Rmsd[g]				
Bond lengths (Å)	0.010	0.009	0.010	0.002
Bond angles (°)	1.18	1.16	1.19	0.58
Dihedral angles (°)	14.7	15.0	14.4	11.7
PDB ID	4ILG	4ILH	4ILJ	4ILI

[a] Data for the highest resolution shell in parentheses

[b] $R_{sym}(I) = \Sigma_{hkl}\Sigma_i |I_i(hkl) - \langle I(hkl)\rangle| / \Sigma_{hkl}\Sigma_i |I_i(hkl)|$; for n independent reflections and i observations of a given reflection; $\langle I(hkl)\rangle$ – average intensity of the i observations

[c] $R = \Sigma_{hkl} ||F_{obs}| - |F_{calc}|| / \Sigma_{hkl} |F_{obs}|$; R_{work} – hkl $\notin$ T; R_{free} – hkl $\in$ T; R_{all} – all reflections; T – test set

[d] ESU – estimated overall coordinate error based on maximum likelihood

[e] A.U. – asymmetric unit

[f] Calculated with MolProbity (http://molprobity.biochem.duke.edu/) (Davis et al. 2004)

[g] Rmsd – root-mean-square deviation from target geometry

Supplemental Table S2. Parameters of proteins used in this study

Protein	Molar extinction coefficient, 280 nm (M^{-1} cm^{-1})	Molecular mass (Da)	T_m (°C)
Aar2p	**54,780**	**42,753**	**45.61**
Aar2p$^{S253E/T345E}$	54,780	42,823	42.48
Aar2p^{M195A}	54,780	42,693	47.18
Aar2p$^{M195A/R186A}$	54,780	42,607	43.54
Aar2p^{R186A}	54,780	42,667	43.75
Aar2p^{S253E}	54,780	42,794	40.70
Aar2p^{Y352A}	53,290	42,660	45.58
Aar2p$^{R55A/I282A}$	54,780	42,626	40.25
Aar2p^{T345E}	54,780	42,780	46.54
Aar2p$^{1-318,\Delta loop}$	50,310	39,963	50.24
Aar2p$^{1-318,\Delta loop,S253E}$	50,310	37,004	43.88
Aar2p^{L350A}	54,780	42,711	46.16
RH	**37,930**	**29,650**	**44.03**
RH^{W1911A}	32,430	29,535	41.30
RH^{V1946A}	37,930	29,622	43.43
RH$^{V1862A/N2068A}$	37,930	29,579	37.45
Jab1	**36,900**	**30,461**	**32.84**
Jab1^{Y2170A}	35,410	30,369	28.68
Jab1^{L2161A}	36,900	30,419	32.61
Jab1^{linker}	**38,390**	**36,333**	**33.30**
CTF	**76,445**	**65,592**	**33.22**
CTF^{Y2170A}	74,955	65,499	29.91
CTF^{L2161A}	76,445	65,550	31.04
Brr2p[a]	**254,750**	**250,975**	**44.03**

[a] wt proteins in bold

Supplemental Table S3. Effects of overexpressing mutant Aar2p proteins and Prp8p C-terminal fragments at 18°C[a]

Prp8p	E3	E3H
Aar2p		
S253A	-	-
S253D	+	+
S253E	+	+
T274A	-	+++
T274D	-	+++
T274E	--	-
Y328A	-	++
Y328E	--	-
S331A	-	
S331D	n.t.	n.t.
S331E	-	-
T345A	-	+++
T345D		+++
T345E		++

[a] + = better growth than wt at 18°C
- = less growth than wt at 18°C
blank = growth like wt at 18°C
n.t. = not tested

Supplemental Figures

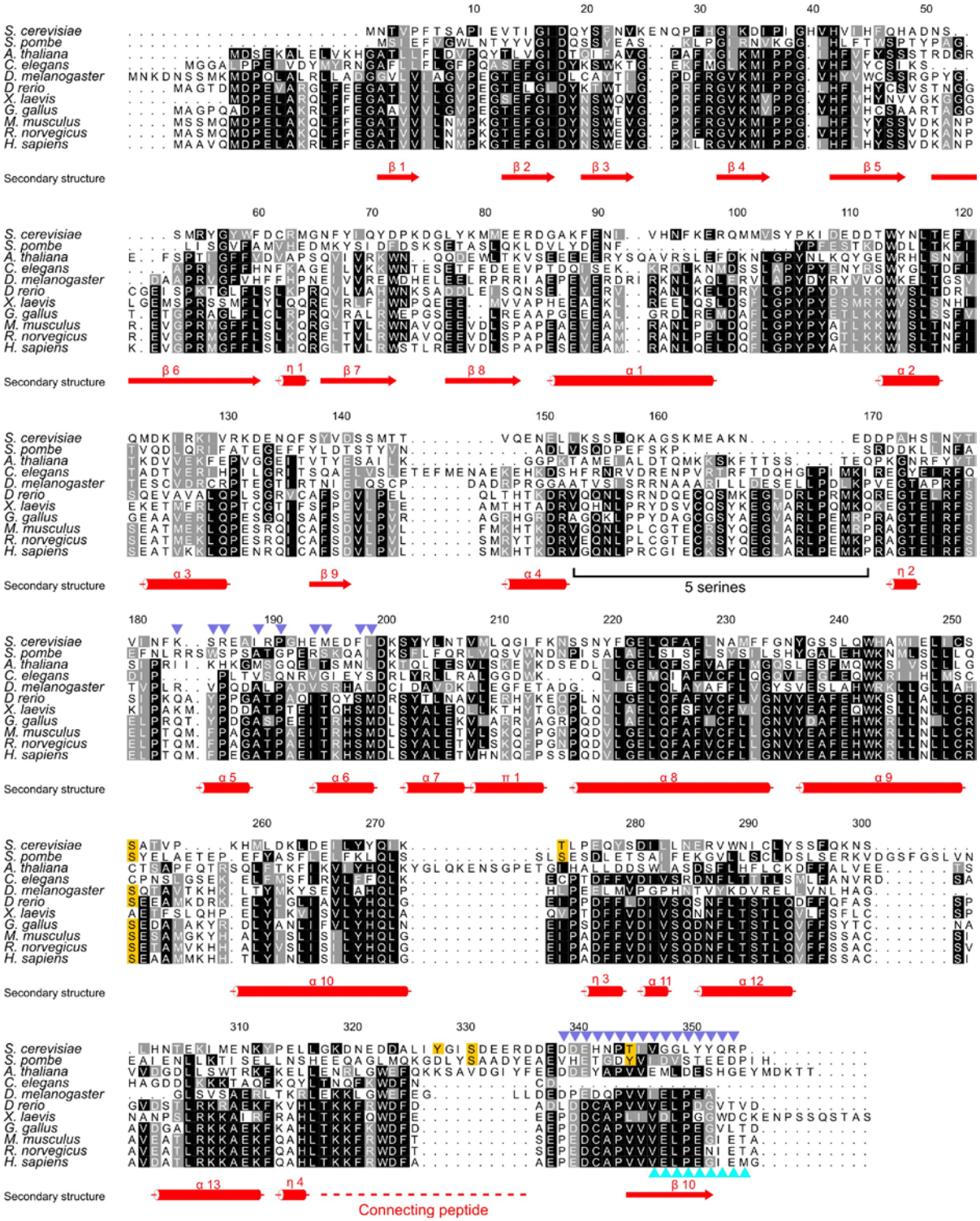

Supplemental Figure S1. Multiple sequence alignment of yeast Aar2p and putative orthologs

The alignment was prepared by ClustalX2 (Larkin et al. 2007) and shaded with ALSCRIPT (Barton 1993). Organisms are identified on the left of the aligned sequences. Higher conservation is indicated by a darker background. Numbering above the alignment refers to yeast Aar2p. Below the alignment, secondary structure elements of yeast Aar2p as detected with PROMOTIF (Hutchinson and Thornton 1996) in the Aar2p$^{\Delta loop}$-RH-Jab1 complex structure are shown in red and are labeled. A dashed red line below the alignment indicates the flexible peptide connecting the globular portion of Aar2p to the C-terminal ß-sheet. A bracket below the alignment refers to the residues that were replaced by five serines in Aar2p$^{\Delta loop}$. Blue triangles above the alignment indicate residues of Aar2p$^{\Delta loop}$, which are in contact to RH. Cyan triangles below the alignment mark residues of Aar2p$^{\Delta loop}$ that form an interface with Jab1. Phosphorylation sites are shaded gold.

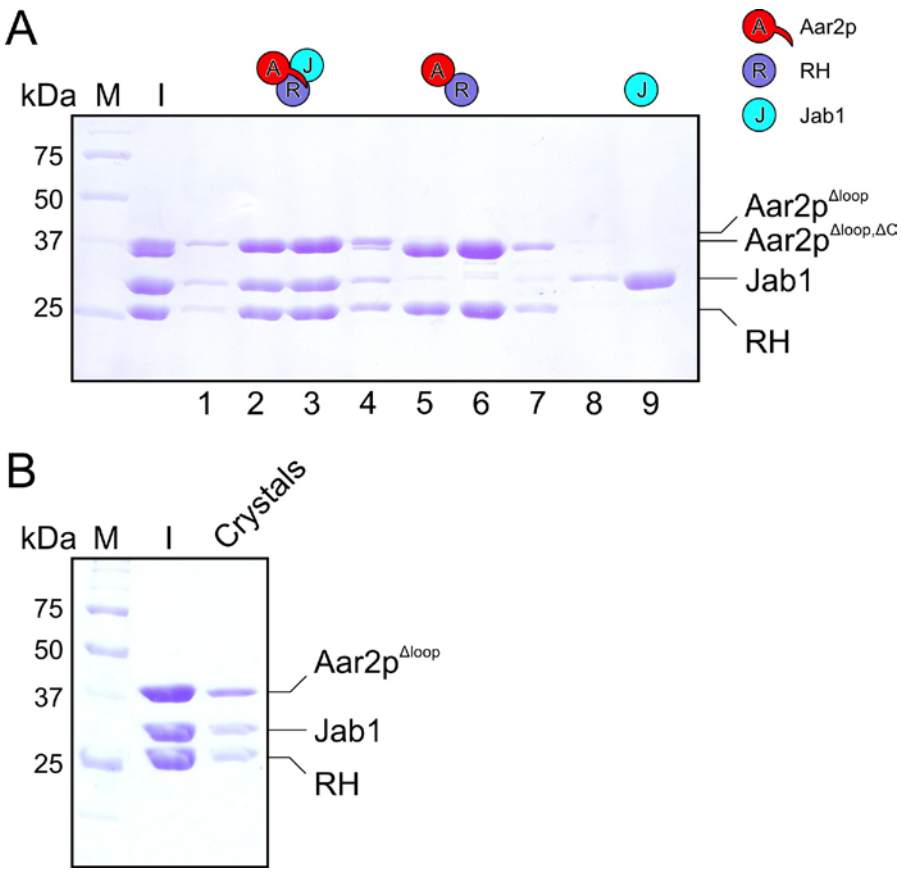

Supplemental Figure S2. Purification and crystallization of a Aar2p$^{\Delta loop}$-RH-Jab1 complex

(*A*) SDS PAGE analysis of a preparative gel filtration run of the Aar2p$^{\Delta loop}$-RH-Jab1 complex. The first two lanes show the protein standard (M) and the gel filtration input (I). Lane numbers below the gel correspond to collected gel filtration fractions. Excess Jab1 eluted last (lane 9). Aar2p$^{\Delta loop}$-RH preparations consistently contained a protein of lower molecular mass than Aar2p$^{\Delta loop}$ (input and lanes 5-6). Similarly, a contaminant slightly shorter than Aar2p was consistently observed during purification of the Aar2p-RH complex. We suspect that this protein corresponded to Aar2p$^{\Delta loop}$ (or Aar2p), which had been C-terminally truncated by endogenous proteases (Aar2p$^{\Delta loop,\Delta C}$), as we had previously observed protease sensitivity in the C-terminal part of Aar2p (Weber et al. 2011). Although co-purifying with the Prp8p RH domain, RH-complexes of these shorter proteins failed to bind Jab1 (lanes 2-3). While presently co-purification with RH is the only indication that the shorter contaminant is an

Aar2p$^{\Delta loop}$ (or Aar2p) variant, this interpretation would be consistent with an important role of the Aar2p C-terminus in Jab1 sequestration. Molecular masses of the standard proteins in kDa are indicated on the left, protein names on the right. The contents of the different fractions are indicated schematically above the gel (icons are explained on the upper right). Icons representing the proteins are defined in the upper right. (*B*) SDS PAGE analysis of dissolved and washed crystals of the Aar2p$^{\Delta loop}$-RH-Jab1 complex. Labels as in (*A*).

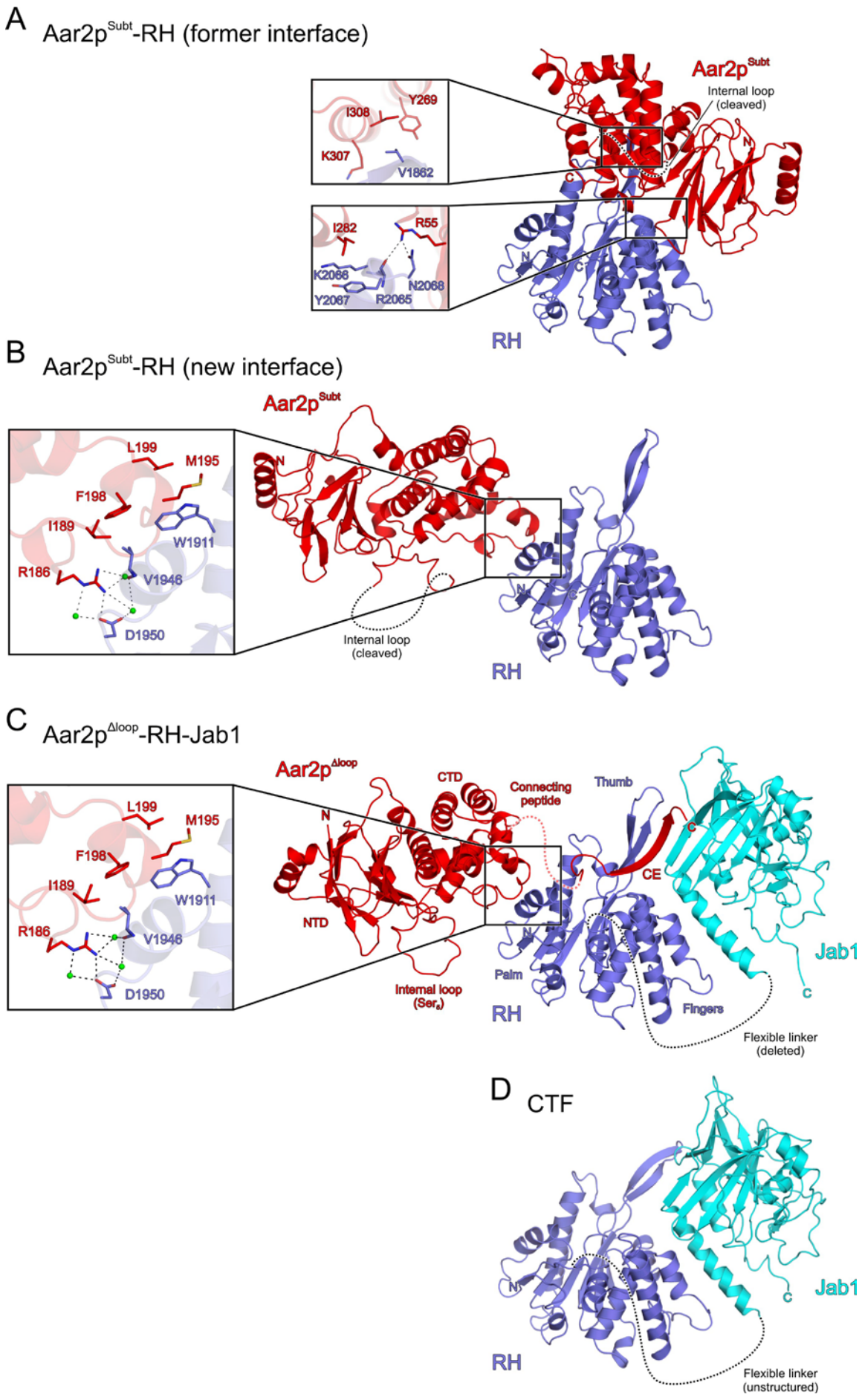
A
Aar2p^Subt-RH (former interface)
Aar2p^Subt
Internal loop
(cleaved)
Y269
I308
K307
V1862
I282
R55
K2068
N2068
Y2067
R2065
RH
B
Aar2p^Subt-RH (new interface)
Aar2p^Subt
L199
M195
F198
I189
W1911
R186
V1948
D1950
Internal loop
(cleaved)
RH
C
Aar2p^Δloop-RH-Jab1
Aar2p^Δloop
CTD
Connecting
peptide
Thumb
CE
NTD
Palm
Fingers
Jab1
Internal loop
(Ser_4)
RH
Flexible linker
(deleted)
D
CTF
Jab1
RH
Flexible linker
(unstructured)

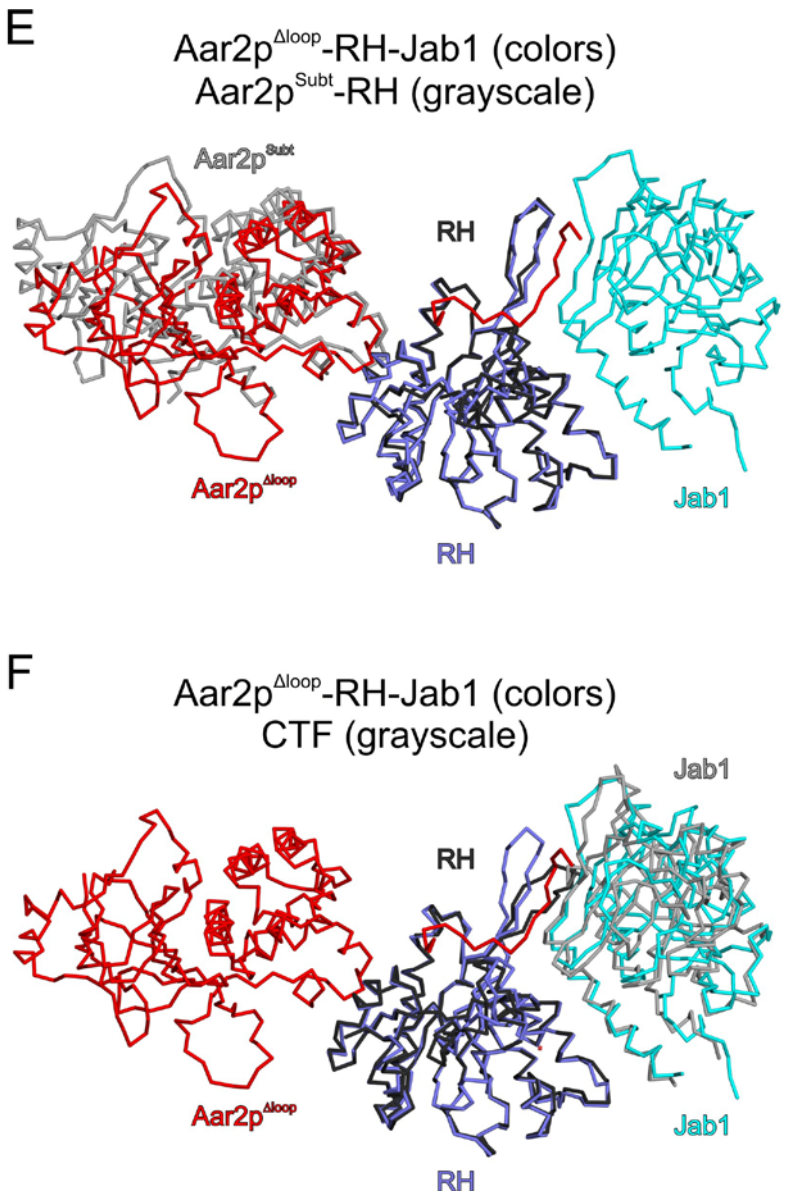

Supplemental Figure S3. Contacts between Aar2p, RH and Jab1 in different crystal lattices

(*A*) Structure of the Aar2p^{Subt}-RH complex as previously assigned (PDB ID 3SBT; Weber et al. 2011). Close-ups – views on two presumed Aar2p^{Subt}-RH contact regions. (*B*) Structure of the Aar2p$^{\Delta loop}$-RH-Jab1 complex as in Fig. 1B with RH domain oriented as in (*A*). Close-up – Aar2p-RH interaction region indicated. (*C*) Alternative interaction between Aar2p^{Subt} and RH in the crystal lattice (Weber et al. 2011) with RH domain oriented as in (*A*). This arrangement is very similar to the Aar2p$^{\Delta loop}$-RH substructure of the Aar2p$^{\Delta loop}$-RH-Jab1 complex. Close-up – Aar2p-RH interaction region indicated. (*D*) Structure of Prp8p CTF (PDB ID 3SBG; Weber

et al. 2011) with RH domain oriented as in (*A*). (*E*) Superposition of the Aar2p$^{\Delta loop}$-RH-Jab1 complex (Aar2p$^{\Delta loop}$ – red; RH – blue, Jab1 – cyan) and the newly assigned Aar2p^{Subt}-RH complex (Aar2p^{Subt} – light gray; RH – dark gray) according to their RH domains. (*F*) Superposition of the Aar2p$^{\Delta loop}$-RH-Jab1 complex (Aar2p$^{\Delta loop}$ – red; RH – blue, Jab1 – cyan) and the CTF structure (RH – dark gray; Jab1 – light gray) according to their RH domains. Colors and labeling as in Fig. 1.

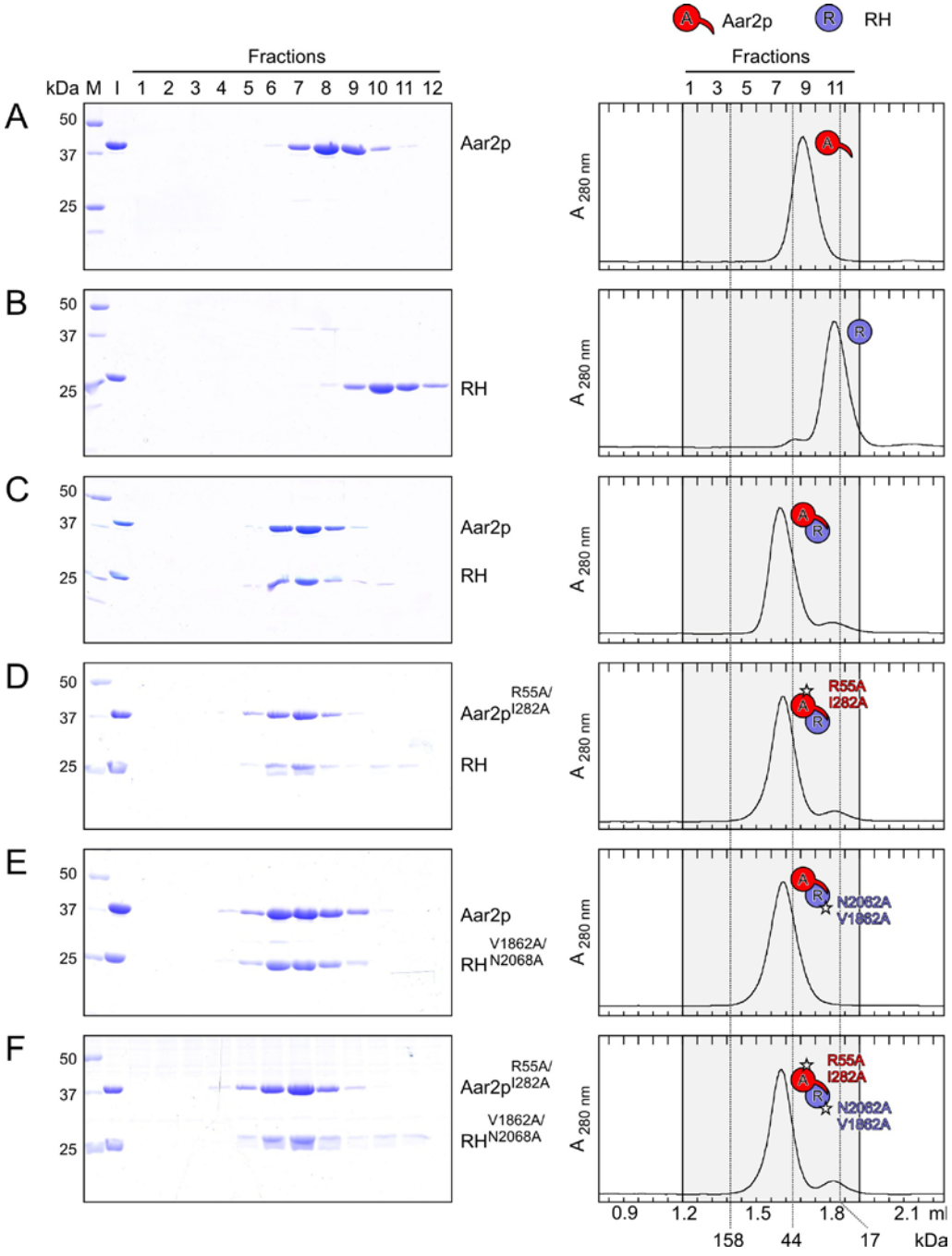

Supplemental Figure S4. Probing of the previously assigned interface of the Aar2p^{Subt}-RH complex

(*A-E*) Gel filtration analyses of the Aar2p-RH protein complex and alanine mutations mapping to the previously assigned Aar2p^{Subt}-RH interface (Weber et al. 2011). Details and labels as in Fig. 2. Icons representing the proteins are defined above the right panels. (*A,B*) Elution of

the isolated wt proteins. (*C*-*E*) Double alanine mutations in Aar2p (R55A/I282A), RH (V1862A/N2068A) or a combination of both still allow complex formation.

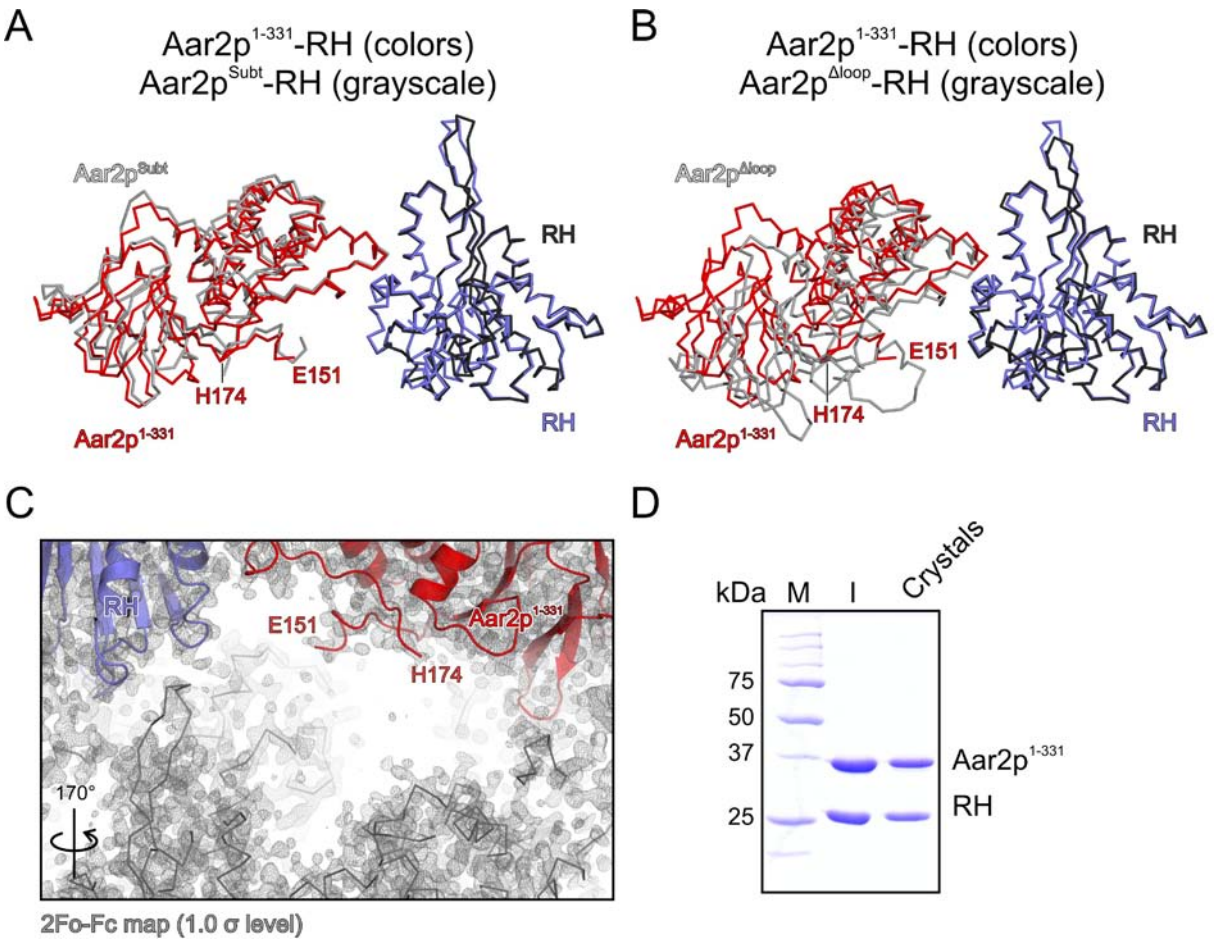

Supplemental Figure S5. The internal loop of Aar2p does not contact RH in the Aar2p$^{1-331}$-RH structure

(*A*) Superposition of the Aar2p$^{1-331}$-RH complex (Aar2p$^{1-331}$ – red; RH –blue) and newly assigned Aar2p^{Subt}-RH complex (Aar2p^{Subt} – light gray; RH – dark gray; PDB ID 3SBT; Weber et al. 2011) according to their RH domains. The last structured residues flanking the internal loop of Aar2p$^{1-331}$ in the Aar2p$^{1-331}$-RH complex are labeled. (*B*) Superposition of the Aar2p$^{1-331}$-RH complex (Aar2p$^{1-331}$ – red; RH –blue) and the Aar2p$^{\Delta loop}$-RH portion of the Aar2p$^{\Delta loop}$-RH-Jab1 complex (Aar2p$^{\Delta loop}$ – light gray; RH – dark gray) according to their RH domains. (*C*) Close up view of the region of the Aar2p$^{1-331}$-RH crystal lattice where the internal Aar2p loop could possibly interact with the RH domain. Symmetry mates are shown as gray ribbons. The final $2F_o$-F_c electron density map is shown as a gray mesh, contoured at

the 1 σ level. Rotation relative to Fig. 1B. (*D*) SDS PAGE analysis of dissolved and washed crystals of the Aar2p$^{1-331}$-RH complex.

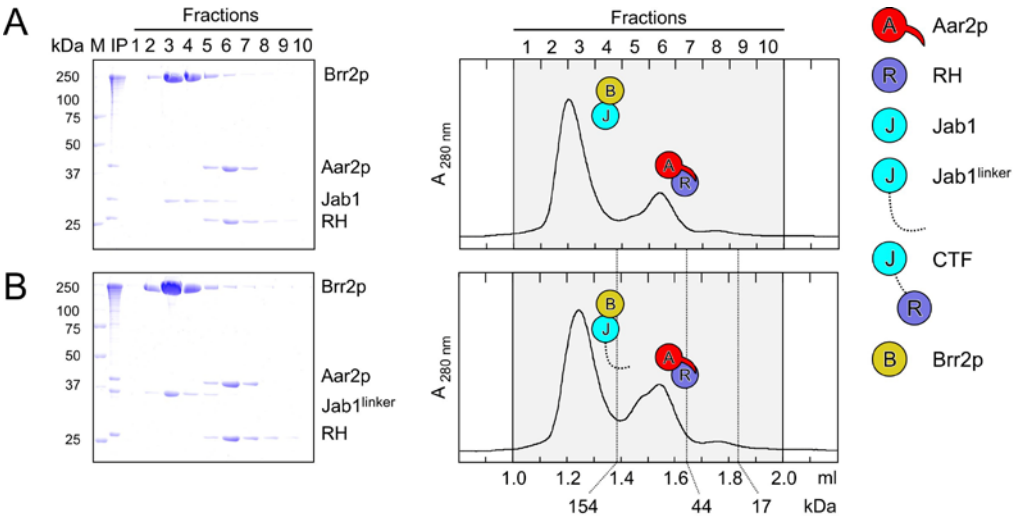
A
Fractions
kDa M IP 1 2 3 4 5 6 7 8 9 10
250
100
75
50
37
25
Brr2p
Aar2p
Jab1
RH
Fractions
1 2 3 4 5 6 7 8 9 10
A 280 nm
B
Aar2p
RH
Jab1
Jab1linker
CTF
Brr2p
B
Brr2p
Aar2p
Jab1linker
RH
1.0 1.2 1.4 1.6 1.8 2.0 ml
154 44 17 kDa

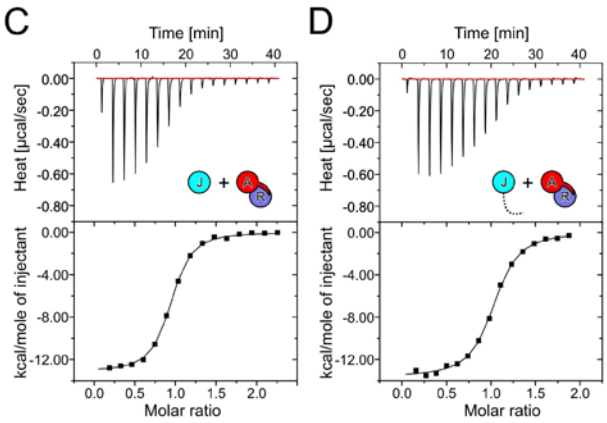
C
Time [min]
Heat [µcal/sec]
kcal/mole of injectant
Molar ratio
N 0.9
Kd 355 nM
ΔH -13.1(kcal mol-1)
ΔS -14.5 (cal mol-1 K-1)
D
Time [min]
Heat [µcal/sec]
kcal/mole of injectant
Molar ratio
N 1.00
Kd 495 nM
ΔH -13.6 (kcal mol-1)
ΔS -16.8 (cal mol-1 K-1)

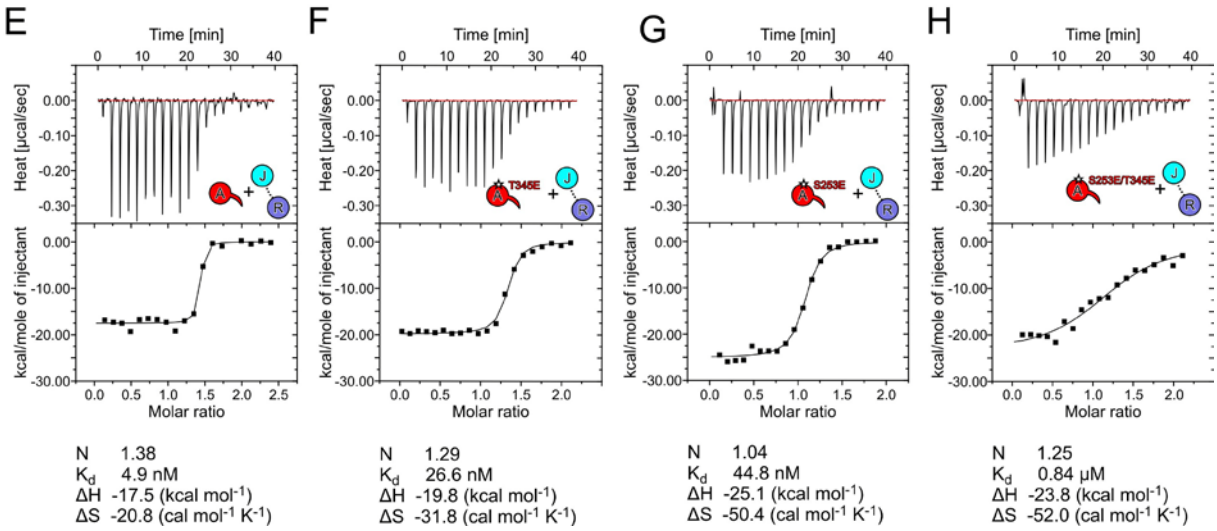
E
Time [min]
Heat [µcal/sec]
kcal/mole of injectant
Molar ratio
N 1.38
Kd 4.9 nM
ΔH -17.5 (kcal mol-1)
ΔS -20.8 (cal mol-1 K-1)
F
Time [min]
T345E
Molar ratio
N 1.29
Kd 26.6 nM
ΔH -19.8 (kcal mol-1)
ΔS -31.8 (cal mol-1 K-1)
G
Time [min]
S263E
Molar ratio
N 1.04
Kd 44.8 nM
ΔH -25.1 (kcal mol-1)
ΔS -50.4 (cal mol-1 K-1)
H
Time [min]
S263E/T345E
Molar ratio
N 1.25
Kd 0.84 µM
ΔH -23.8 (kcal mol-1)
ΔS -52.0 (cal mol-1 K-1)

Supplemental Figure S6. Role of the RH-Jab1 linker

(*A,B*) Gel filtration runs analyzing the effect of the RH-Jab1 linker on competitive binding of Aar2p and Brr2p. Details and labels as in Fig. 2. Icons representing the proteins are defined in the upper right. The linker preceding Jab1 in the Jab1^{linker} construct is indicated by a dashed line. (*C,D*) ITC experiments comparing the titration of preformed Aar2p-RH complex into Jab1 solutions with and without the linker sequence. Thermodynamic binding parameters are listed. (*E-H*) ITC experiments comparing the binding of CTF to wt Aar2p or Aar2p variants bearing the indicated phospho-mimteic mutations. Thermodynamic binding parameters are listed.

A

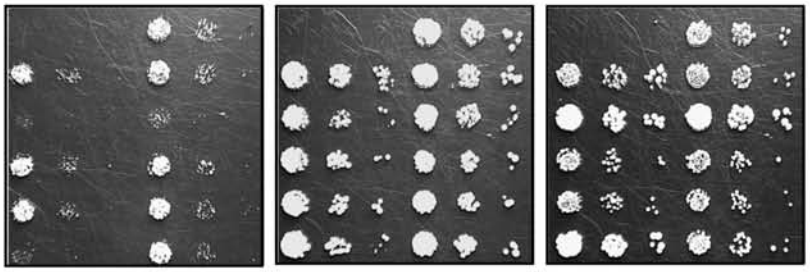

Plate legend

⊠	Y328A
wt	Y328E
S253A	S331A
S253E	S331E
T274A	T345A
T274E	T345E

B

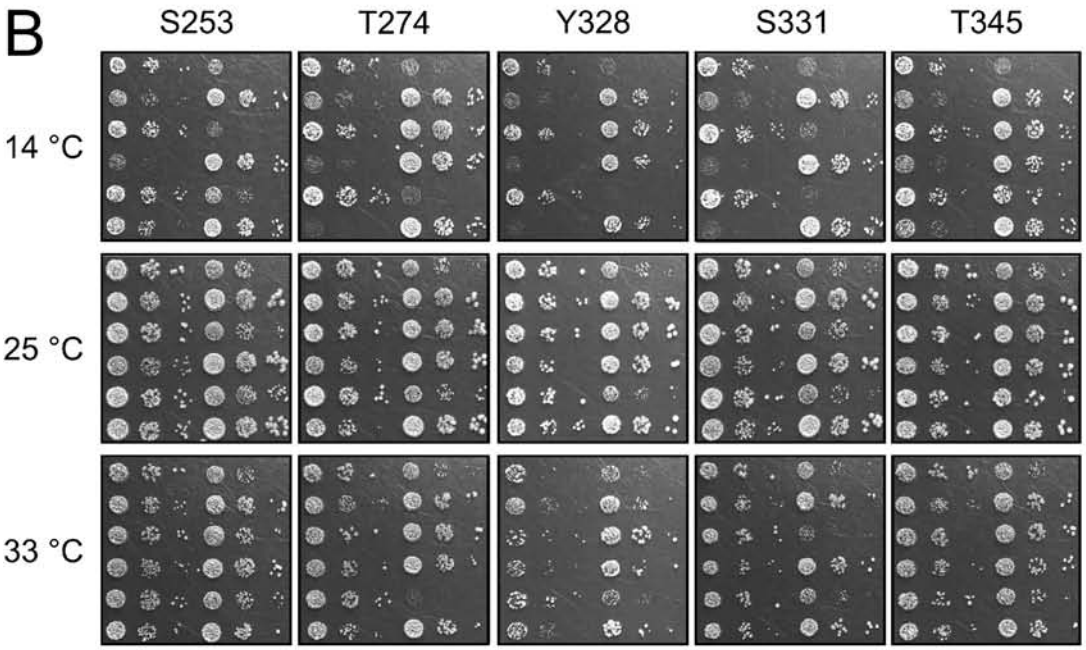

Plate legend

E1	E3H	Aar2p wt
E3	pActII	
E1	E3H	Aar2p with indicated phosphosite mutated to alanine
E3	pActII	
E1	E3H	Aar2p with indicated phosphosite mutated to glutamate
E3	pActII	

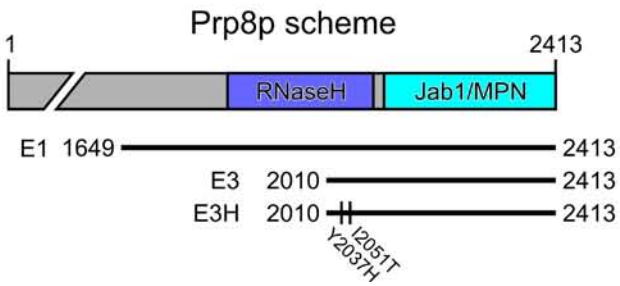

Supplemental Figure S7. Growth phenotypes elicited by Aar2p mutants

(*A*) Growth at different temperatures of yeast cells carrying the indicated *aar2* alleles on their genomes. S253A, S331A and T274E mutations of Aar2p, when present on the genome, cause a cs growth phenotype. Plate legend on the right. (*B*) Effects of alanine and phospho-mimetic aspartate and glutamate mutations of Aar2p when overproduced together with the indicated Prp8p C-terminal fragments. Fragment E3 contains Prp8p residues 2010-2413. Fragment E3H corresponds to fragment E3 but has Y2037H and I2051T mutations that result in enhanced interaction with Brr2p (van Nues and Beggs 2001). Fragment E1 (Prp8 residues 1649-2413) contains additional regions N-terminal of fragments E3 and E3H. A plate legend and a scheme indicating the position of Prp8p fragments are provided on the bottom. Data from these experiments are summarized in Supplemental Table S3.